Myeloma-derived extracellular vesicles mediate HGF/c-Met signaling in osteoblast-like cells

Authors

Olaf Strømme, Department of Clinical and Molecular Medicine, Faculty of Medicine and Health Sciences, Norwegian University of Science and Technology (NTNU), Trondheim, Norway.

Email: olaf.stromme@ntnu.no

Katarzyna M. Psonka-Antonczyk, Department of Physics, Faculty of Natural Sciences, Norwegian University of Science and Technology (NTNU), Trondheim, Norway

Email: katarzyna.psonkaantonczyk@gmail.com

Bjørn Torger Stokke, Department of Physics, Faculty of Natural Sciences, Norwegian University of Science and Technology (NTNU), Trondheim, Norway.

Email: bjorn.stokke@ntnu.no

Anders Sundan, Centre of Molecular Inflammation Research and Department of Clinical and Molecular Medicine, Faculty of Medicine and Health Sciences, Norwegian University of Science and Technology (NTNU), Trondheim, Norway

Email: anders.sundan@ntnu.no

Carl-Jørgen Arum, Department of Clinical and Molecular Medicine, Faculty of Medicine and Health Sciences, Norwegian University of Science and Technology (NTNU), Trondheim, Norway and Department of Urology, St. Olavs University Hospital, Trondheim, Norway

Email: carl-jorgen.arum@ntnu.no

Gaute Brede, Department of Clinical and Molecular Medicine, Faculty of Medicine and Health Sciences, Norwegian University of Science and Technology (NTNU), Trondheim, Norway.

Email: gaute.brede@ntnu.no

Contact information for corresponding author

Olaf Strømme, Arilds gate 2, 7017 Trondheim, Norway

Email: olaf.stromme@ntnu.no

Mob: +47 99376188

Abstract

Multiple myeloma is an incurable cancer of antibody-producing plasma cells. Hepatocyte growth factor (HGF), a cytokine aberrantly expressed in half of myeloma patients, is involved in myeloma pathogenesis by enhancing myeloma growth and invasiveness, and may play a role in myeloma bone disease by inhibiting osteoblastogenesis. In this study, we investigated whether extracellular vesicles (EVs) may play a role in HGF signaling between myeloma cells and osteoblast-like target cells. EVs from the HGF-positive cell line JJN-3 and the HGF-negative cell line INA-6, and from bone marrow plasma and primary human myeloma cells, were isolated using sequential centrifugation techniques and the presence of HGF on the EV-surface was investigated with ELISA. EVs from both cell lines were added to an established bioassay where HGF is known to induce interleukin-11 secretion in osteoblast-like cells. Our results show that HGF was bound to the surface of JJN-3-derived EVs, while INA-6-derived EVs were negative for HGF. Only JJN-3-derived EVs induced IL-11 secretion in osteoblast-like recipient cells. When osteoblast-like cells were preincubated with a specific HGF-receptor (c-Met) inhibitor, no induction of interleukin-11 was observed. Downstream c-Met phosphorylation was demonstrated by immunoblotting. EVs isolated from bone marrow plasma and primary myeloma cells were HGF-positive for a subset of myeloma patients. Taken together, this work shows for the first time that HGF bound on the surface of myeloma-derived EVs can effectuate HGF/c-Met signaling in osteoblast-like cells. Myeloma-derived EVs may play a role in myeloma bone disease by induction of the osteoclast-activating cytokine interleukin-11 in osteoblasts.

Keywords

Extracellular vesicles; Hepatocyte growth factor; c-Met; multiple myeloma; osteoblast; interleukin-11

Abbreviations

AFM: Atomic force microscopy **ELISA**: Enzyme-linked immunosorbent assay **BMP:** Bone marrow plasma **EV**: Extracellular vesicle **FCS:** Fetal calf serum **FITC**: Fluorescein isothiocyanate **HGF**: Hepatocyte growth factor **hrHGF** Human recombinant HGF **HSBD**: Heparan sulphate binding domain **IL-11:** Interleukin-11 **MBD**: Myeloma bone disease **MM:** Multiple myeloma **NTA**: Nanoparticle tracking analysis **PI:** Proprium iodide **PM:** Plasma membrane **PBS**: Phosphate buffered saline **TBST** Tris-buffered saline and Tween 20 **TGF-beta:** Transforming growth factor-beta

Introduction

Multiple myeloma (MM) is an incurable cancer of antibody-producing plasma cells. Hepatocyte growth factor (HGF) is involved in myeloma pathogenesis by enhancing tumor cell proliferation, motility and migration (1-4). The pleiotropic effects of HGF are initiated upon binding to its proto-oncogenic c-Met receptor, which is expressed by several malignant as well as non-malignant cell types, including myeloma cells and osteoblasts (5-7). HGF serum concentrations are elevated in approximately half of MM patients, conferring a poorer prognosis (8, 9). HGF may also play a role in the pathogenesis of myeloma bone disease (MBD), a condition characterized by increased osteoclast activity combined with osteoblast dysfunction, by antagonizing bone morphogenic protein-induced osteoblastogenesis (10). Furthermore, HGF expression in the bone marrow microenvironment of MM patients is correlated with the extent of bone disease (11).

While the interplay between myeloma cells and osteoblasts has been thoroughly investigated (12, 13) , the role of extracellular vesicles (EVs) as signaling mediators in myeloma-osteoblast interactions is largely unexplored. Exosomes are small EVs (30–120 nm in diameter) originating from endocytic multivesicular compartments. They are released upon fusion of these compartments with the plasma membrane (PM), keeping many of the PM-associated factors in the same orientation on EVs as on the PM (14, 15). While sharing many of its characteristics with exosomes, microvesicles are more heterogenic in size (50–1000 nm in diameter) and are released from the cell surface by a budding process from the PM (16, 17). The abundance of

signaling proteins and adhesion molecules at the EV surface facilitates EV-mediated intercellular communication, both in physiological and pathological conditions (18-22).

Myeloma-derived EVs have been reported to express both HGF and the proteoglycan syndecan-1 on their membrane surface (23). HGF is known to bind to proteoglycans such as syndecan-1 through heparan sulfate binding domains (HSBD) (24, 25). In this study, we hypothesize that EVs derived from HGF-secreting myeloma cells harbor HGF bound to proteoglycans at the EV surface and that EV-bound HGF can effectuate c-Met signaling in osteoblast-like recipient cells. In this work, we suggest a novel mechanism for signaling between myeloma cells and osteoblasts. Improved understanding of myeloma signaling may enable the development of more targeted therapies.

Materials and methods

Cell cultures

The human osteosarcoma cell lines U2OS and Saos-2 were obtained from the American Type Culture Collection (Rockville, MD, USA). The human myeloma cell line JJN-3 was kindly provided by Dr. J. Ball (Department of Immunology, University of Birmingham, UK). INA-6, also a human myeloma cell line, was a kind gift from Dr. M. Gramatzki (Erlangen, Germany). JJN-3 and INA-6 cell lines were cultured in RPMI 1640 (GIBCO), supplemented with 10 % EV-depleted fetal calf serum (FCS), 2 mmol/L glutamine, and 40 µg/mL gentamycin. As the INA-6 cell line is IL-6 dependent, recombinant human IL-6 (Sandoz, Basel, Switzerland) was added to the INA-6 medium (1 ng/ml). U2OS and Saos-2 cells were cultured as described above except that only 2 % EV-depleted FCS was used in order to minimize the contribution of soluble cytokines from FCS for the downstream HGF bioassay. Primary human MM cells were cultured in RPMI 1640, supplemented with 10% EV-depleted human serum, 2mg/ml IL-6, 2 mmol/L glutamine, and 40 µg/mL gentamycin.

Preparation of bone marrow plasma

Bone marrow aspirates were obtained from patients admitted to the Section of Hematology, St. Olav's Hospital, Trondheim, Norway, after approval from the regional ethics committee and informed consent from patients. Bone marrow aspirate was transferred to labelled CPT tubes and centrifuged at 1500 × g at 20 °C for 30 minutes. The mononuclear cells were recognized as a white matter just above the gel and a separate procedure was used for further processing of

these cells. The supernatant (bone marrow plasma) was pipetted into a new Falcon tube (14 ml) and frozen at −20 °C for storage.

EV isolation

Isolation of EVs from myeloma cell cultures and bone marrow plasma was performed using sequential centrifugation and ultracentrifugation adapted from the previously reported procedure (26). Cell lines and primary human MM cells were cultured for 24 and 72 hours respectively, in media supplemented with EV-depleted serum before EV isolation. Cells were first pelleted by centrifuging at 300 × g for 10 minutes and the subsequent supernatant centrifuged at 12 000 × g for 45 minutes. The resulting supernatant was then ultracentrifuged at 100 000 × g for 90 minutes (Polyallomer tubes, Beckman). The pellet was resuspended in ~15 ml of phosphate buffered saline (PBS) and filtered with a 0.22 μm pore size filter (Millipore). Bone marrow plasma-derived EVs were pelleted by a final ultracentrifugation step at 100 000 × g for 90 minutes. To prevent contamination with soluble HGF, cell culture samples were subjected to three additional ultracentrifugation/resuspension steps. Pellets were resuspended in 250 μL of RPMI 1640 (cell culture samples) or PBS (bone marrow plasma) before being aliquoted and stored at −80 °C. All centrifugation steps and solutions were stored at 4 °C.

Depletion of EVs from FCS

To obtain a pure myeloma cell-derived EV-fraction not contaminated by serum-derived EVs, both FCS and human serum were subjected to differential centrifugation as described above except that only one ultracentrifugation step was performed, overnight at 100 000 × g, for the

complete removal of EVs. The final supernatant was frozen (−20 °C) in aliquots and used as EV-depleted serum.

Nanoparticle Tracking Analysis

The size distributions and concentrations of EV samples were determined with nanoparticle tracking analysis (NTA) (Nanosight LM10 equipped with 40 mW laser with wavelength 638 nm, Nanosight Ltd., Amesbury, UK). To minimize EV-aggregation, samples were vortexed for 5 seconds followed by thorough pipetting. To assure enough volume to load samples into the measuring chamber, all samples were diluted to a volume of 300 μl using PBS. Additional dilutions with PBS were made to match the concentration within the instrument detection range if needed. The recording time was chosen to be 90 seconds. Automated analysis of recorded video was performed in NTA analytical software. To ensure equal concentrations of JJN-3 and INA-6-derived EVs for use in downstream applications, normalized stock solutions were made by dilution of aliquots with RPMI 1640 based on concentrations as measured by NTA, and stored at −80 °C (referred to as EV stock solutions).

Atomic force microscopy

Aliquots of EV samples were diluted 10-fold in PBS, and deposited on glutaraldehyde-functionalized mica surface prepared as reported (27). A 15 μL aliquot of the aqueous EVs was deposited onto the glutaraldehyde-modified mica and incubated for 30 minutes in humid environment, subsequently rinsed with PBS and mounted for atomic force microscopy (AFM) imaging. Vesicles were imaged employing a MultiMode 8 (Bruker AXS Inc., Madison, USA) in

ScanAsyst mode and using ScanAsyst-fluid probes (0.7 N m^{-1}, resonance frequency 150 kHz). Imaging was performed in PBS and images with 512×512 pixels collected.

Silverstaining

Protein extracts from identical volumes of JJN-3 and INA-6-derived EVs (3 µL from EV stock solutions) were subjected to SDS-PAGE and silverstained according to the protocol of the ProteoSilver™ Silver Stain Kit (Sigma).

Flow cytometry

To measure cell viability, cells were incubated with annexin V fluorescein isothiocyanate (FITC) (0.2 µg/mL in 1 × annexin binding buffer) for 1 h on ice. Propidium iodide (PI) (1.4 µg/mL) was added 5 min prior to data acquisition using an LSRII flow cytometer (BD Biosciences). Cells negative for both annexin V and PI staining were considered viable.

HGF and IL-11 quantification

HGF protein concentrations were quantified for JJN-3- and INA-6-derived EVs using the DuoSet ELISA Development kit (R&D Systems, Minneapolis, MN, USA). Assay was performed according to manufacturer's protocol in EV coated wells. HGF protein concentrations for BMP samples, BMP-derived EVs and primary MM cells were quantified using the Human HGF ELISA kit (ab100534; Abcam). IL-11 was measured by ELISA as previously described (28).

HGF bioassay

U2OS and Saos-2 cells were split the day before the assay in 96 wells flat bottom plates (Costar) at ~70 % confluence and cultured overnight to reach confluence at assay start (approximately

$4x10^4$ cells/well). Cells were washed with RPMI 1640 twice and given fresh media. JJN-3 and INA-6-derived EVs were added from stock solutions in two concentrations: low dose (1 × cons) ~6×10^6 EVs/ml and high dose (3 × cons) ~1.8×10^7 EVs/ml. To avoid EV-aggregation, EVs were resuspended in RPMI 1640 and filtered through a small volume 0.22 µm syringe filter (Millipore) immediately before addition to cell culture. Human recombinant HGF (hrHGF) was added at a concentration of 200 ng/ml for U2OS cells and 100, 200 and 300 ng/ml for Saos-2 cells. When a c-Met inhibitor was used, cells were incubated with 50 nM (final concentration), PHA 665752 (Pfizer, San Diego, CA, USA) in assay media for 20 minutes before addition of EVs or human recombinant HGF. 100 µL of ultracentrifugation supernatant was used. U2OS and Saos-2 culture media was harvested 8 hours after assay start and subsequently quantified for IL-11 using ELISA.

Heparin treatment of bead-bound EVs

Purified EVs (excess) were prebound to anti-CD9 antibody coupled magnetic Dynal beads (Invitrogen # 10606D). Binding was performed with 20 µL of magnetic beads that were washed twice by adding 200 µL RPMI buffer, mixed for 30 seconds and placed on the magnet for 1 minute before discarding the supernatant. Purified EVs in RPMI was added (100 µL final volume) to the magnetic beads and mixed well. The tube was then incubated 5 hours at 4 °C on rotation. The tubes were then centrifuged for 5 seconds to collect the sample at the bottom of the tube and the bead-bound EVs were washed by adding 300 µL RPMI. The samples were mixed gently by pipetting and the tube placed on the magnet for 1 minute before discarding the supernatant. The remaining bead-bound EVs were resuspended in 100 µL RPMI with EV-depleted 2 % FCS. The EV-loaded magnetic beads were incubated for 5 minutes at room

temperature in a solution consisting of 40 µg/ml heparin in RPMI 1640 on rotation, then introduced onto the magnet (DynaMag Spin). After 1 minute on the magnet the supernatant was removed, and the beads were incubated with a second round on Heparin/RPMI 1640 on rotation at room temperature for 5 minutes before magnetic separation. Finally, the EV-loaded beads were washed twice using the same procedure but with RPMI 1640 only to get rid of excess heparin.

Phospho-c-Met signaling assay

U2OS cells were grown in six-well culture plates for 24 hours in serum-free media before incubation with EVs isolated from JJN-3 and INA-6 cells, both at a concentration of ~6×10^6 EVs/ml. hrHGF was added at a concentration of 50 ng/ml. Cells were harvested for lysis after eight minutes of incubation.

Immunoblotting

For western blot analysis, cells or aliquots from EV stock solutions were lysed in Complete-M Lysis Buffer (Roche) for 20 min at 4 °C. Nuclei and cell debris were removed by centrifugation. EVs solubilized in lysis buffer or post-nuclear lysates were quantified by Bradford assay, solubilized in Laemmli loading buffer and analyzed under reducing conditions by SDS-PAGE. For the phospho-c-Met signaling assay, U2OS cells were lysed in RIPA buffer with 1 mM dithiothreitol and 4x LDS sample lading buffer (Novex Bolt) was used. Proteins were transferred to a nitrocellulose-membrane using the iBlot system (Invitrogen) according to manufacturer's protocol. The blot was blocked with a 5 % dry milk and 0.05 % tween-20 in tris-buffer saline (TBST) for 45 minutes, before addition of primary antibody in TBST at the dilution

recommended by the manufacturer, overnight at 4 °C. The blot was washed 3 times for 10 minutes in TBST before incubation with the appropriate secondary IRDye-800cw-labeled antibody for 40 minutes at room temperature. After four washes in TBST, the membranes were developed using the Li-Cor system.

Antibodies used: α-CD9 (Abcam), α-Alix (sc-53540, Santa Cruz), α-HGF (Polyclonal goat, R&D), α-IL-11 (R&D), α-LAMP-1 (D2D11, Cell Signaling), and α-PDI (mAb Cell Signaling), α-Phospho-Met (mAb #3077, Cell Signaling). Secondary antibodies: Goat-anti-mouse IRDye-800cw and Goat-anti-rabbit IRDye-800cw (both from Odyssey). All antibodies were used at the recommendations of the manufacturer.

Statistical analysis

Statistical analysis for the ELISA analysis was performed with the GraphPad Prism software.

Results

Characterization of EVs secreted by JJN-3 and INA-6 myeloma cell lines

The size distribution of EVs was determined by NTA (Figure 1A). EVs from both cell lines showed analogous but not identical distribution with sizes in the range 50–350 nm. AFM analysis revealed sizes with respect to full width at maximum height in the range 100–150 nm, and heights from 15 to 40 nm (Figure 1B). The presence of EV-markers was assessed within EV-isolates from both JJN-3 and INA-6 cells using immunoblotting (Figure 1C). The EV-markers Alix, CD9 and LAMP-1 were present in EVs from both myeloma cell lines. Silverstained protein gels showed that EVs from both cell lines had similar protein expression levels (Figure 1D).

JJN-3-derived EVs present HGF on their vesicle surface

An HGF-specific ELISA was performed to evaluate the presence of HGF in EVs from JJN-3 and INA-6 cells (from EV stock solutions). HGF was only found to be present on the surface of JJN-3-derived EVs (Figure 2A).

JJN-3-derived EVs induce IL-11 secretion through the c-Met receptor in osteoblast-like recipient cells

To assess whether JJN-3-derived EVs mediated HGF/c-Met signaling we used an established bioassay where HGF is known to induce IL-11 secretion in osteoblast-like cells in a dose-dependent manner (28). Equal and adequate cell viability for the two cell lines used in the bioassay was confirmed (Figure 1E). EVs were added to U2OS cells from stock solutions in two concentrations, low dose (1 × cons) ~$3x10^5$ EVs/well and high dose (3 × cons) ~$9x10^5$ EVs/well.

JJN-3 derived induced IL-11 secretion in U2OS cells, in a dose dependent manner. Incubation with INA-6-derived EVs showed no dose-response dependency. To determine whether the induction of IL-11 secretion was a result of activated c-Met signaling, U2OS cells were preincubated with a c-Met inhibitor before adding JJN-3-derived EVs. In the presence of the c-Met inhibitor, IL-11 secretion was reduced to background levels (Figure 2B). To ensure that these results were not restricted to U2OS cells, we performed additional experiments in another osteoblast-like cell line, the osteosarcoma cell line Saos-2, obtaining similar results (Figure 2D).

Il-11 induction is reduced after heparin treatment of JJN-3-derived EVs

Since HGF contains a HSBD, treatment of HGF-positive EVs with heparin should lead to a displacement of HGF from the surface of EVs (29, 30). Heparin treated and non-treated HGF-bead-bound EVs were added separately to U2OS cells and IL-11 culture media level measured. A significantly lower IL-11 secretion in U2OS cells was observed with heparin-treated EVs compared to non-treated EVs (Figure 2C).

C-Met in U2OS cells is phosphorylated in response to JJN-3-derived EVs

To investigate whether c-Met was phosphorylated in response to JJN3-derived EVs, U2OS cells were incubated with JJN-3-derived EVs, INA-6-derived EV and hrHGF. Immunoblotting against c-Met phosphorylated at the tyrosine residues 1234/1235 shows a band at 145 kilodalton for U2OS cells incubated with JJN-3-derived EVs and hrHGF, while incubation with INA--derived EVs, ultracentrifugation supernatant failed to produce this band (Supplementary Figure 1).

HGF-positive EVs are found for a subset of myeloma patients

An HGF-specific ELISA was performed to investigate whether EVs from BMP of MM patients and cultured primary myeloma cells express HGF (Figure 3). Additionally, ELISA was performed for the BMP samples, of which the EVs were derived. ELISA results show that HGF-positive BMP-derived EVs were found for a subset of patients. A partial correlation between HGF values for BMP and BMP-derived EVs seem to be observed. Patient 9 and 21 seem to express relatively high values of HGF for both BMP-derived EVs and BMP. However, patient 20 express high HGF values for BMP, but only just over the assay's detection limit of 3 pg/ml for BMP-derived EVs. Concerning EVs isolated from cultured primary MM cells, only patient 8 express HGF values consistently above the assay's detection limit. The size distribution for EVs isolated from BMP and primary myeloma cells were measured by NTA (Supplementary Figure 2B and 2C).

Discussion

HGF has previously been shown to induce IL-11 secretion in osteoblast-like cells both as soluble and cell-surface bound factor (28). Furthermore, a complex of HGF and shed syndecan-1 found in cell culture media, as well as in pleural effusions from myeloma patients, has been demonstrated to induce IL-11 secretion in osteoblast-like cells through c-Met activation (31, 32). Based on the findings of the present study, we propose that EV-mediated HGF/c-Met signaling constitute a previously undescribed signaling mechanism (Figure 4).

Our findings indicate a role for myeloma-derived EVs in the pathogenesis of MBD. As suggested by Hjertner et al. (28), an increased IL-11 level in the bone marrow microenvironment may

favor bone degradation, as IL-11 is known to stimulate osteoclastogenesis and inhibit bone formation *in vitro* (33-35). IL-11 has also been demonstrated to induce osteoclastogenesis and osteolytic bone lesion formation *in vivo* (36). A role for MM-derived EVs in MBD pathogenesis has been explored by other authors. Raimondi et al found that MM-derived exosomes induced osteoclastogenesis as well as an increased resorbing capacity of osteoclasts (37). A recent paper by Menu et al demonstrate that MM-derived exosomes may contribute to MBD both by enhancing osteoclast activity and by inhibiting osteoblast differentiation (38). Other studies have found a role for MM-derived EVs in various pathogenic processes of MM, such as enhanced angiogenesis (39, 40), myeloma cell proliferation (41) and invasiveness (23, 42). Additionally, EVs derived from neighboring stromal cells may modulate MM growth (43, 44). Recently, it was shown that mesenchymal stromal cells could contribute to MM cell proliferation through EV-mediated transfer of the long non-coding RNA LINC00461, which relieves the inhibitory effects of microRNAs mir-15a and mir16 on the proto-oncogene bcl-2 (45).

We were not able to show direct evidence of HGF binding on the EV surface by electron microscopy. However, several lines of evidence indicate that HGF is bound to the surface of myeloma-derived EVs. Firstly, our ELISA demonstrates that JJN-3-derived EVs are positive for HGF. To minimize the chance of this being co-pelleted HGF in the EV-fraction, two additional and sequential washing/ultracentrifugation steps were performed compared to standard EV-isolation protocol to avoid carry-over of soluble (non-EV associated) HGF. Secondly, the supernatant from the last ultracentrifugation step when isolating JJN3-derived EVs did not induce IL-11 secretion, implying that the supernatant was essentially negative for HGF.

Furthermore, heparin treatment of EVs significantly reduced IL-11 secretion, suggesting that HGF is at least partially bound to proteoglycans on the EV surface. It has been reported that heparin may affect EV-cell interactions (23, 46). We argue, however, that heparin displacement of HGF is a more likely explanation for reduced IL-11 secretion than general inhibition of EV-cell interactions, especially considering the differences in methodology, where we have attempted a thorough removal of excess heparin. Additionally, heparin displacement of HGF from proteoglycans is well documented (29, 30), as demonstrated several times in the same HGF bioassay (28, 31, 32).

Characterization of EVs from BMP and cultured primary myeloma cells has to our knowledge previously not been performed. We investigated the presence of EVs in bone marrow plasma from six patients suspected of MM, by NTA and immunoblotting (Supplementary Figure 1A). We then isolated EVs from BMP from fifteen additional MM patients and an HGF-specific ELISA showed that a subset of patients express HGF-positive EVs. We also investigated the presence of HGF-positive EVs isolated from cultured primary MM cells for six patients. EVs derived from one of the six patients express HGF above the assay's detection limit. While studies for a larger number of patients is needed, these results indicate that MM-patient-derived EVs may express HGF, and EV-mediated HGF-signaling could potentially be operative *in vivo.*

Previously, EVs have been reported to mediate signaling for a limited number of cytokines, among them interferon gamma (47), heat shock protein 70 (48), amphiregulin (49) and transforming growth factor-beta (TGF-beta) (50). For the latter, it was shown that prostate cancer-derived exosomes induced differentiation of fibroblasts to a proto-oncogenic

myofibroblastic phenotype through TGF-beta on the exosome surface. This finding could not be replicated with soluble TGF-beta, highlighting the significance of EVs as mediators of TGF-beta signaling (51). The relative importance of EV-mediated HGF signaling to previously described signaling modalities is currently unknown. Likewise, it remains unclear whether EV-mediated HGF signaling may lead to distinct downstream signaling patterns. Future experiments addressing differences in the stability and potency of EV-mediated versus non-EV-mediated HGF-signaling could further highlight the role of HGF-positive EVs during development of myeloma.

Conclusion

Myeloma-derived EVs harbor HGF on their surface that is functional in HGF/c-Met signaling in osteoblast-like cells. HGF-positive EVs may play a role in MBD through induction of the osteoclast-activating cytokine IL-11 in osteoblasts. Given the emerging acknowledgement of the role of EVs in intercellular signaling, and the abundant presence of EVs in the bone marrow, a further understanding of EV-mediated signaling may be central in understanding myeloma pathogenesis.

Declarations

Ethics approval and consent to participate

All use of patient material is approved by Regional Ethic Committee (REK). REK: 2009/1317-7 and REK:2011/2029. All patients gave informed consent in accordance with the Declaration of Helsinki.

Availability of Data and Materials

All data generated or analyzed during this study are included in this published article (and its supplementary information files).

Competing interests

The authors claim no competing interests.

Funding

This study was supported by grants from Central Norway Regional Health Authority (GB, KMPA and BTS), The Research Council of Norway to KMPA and BTS through the Norwegian Micro- and Nano-Fabrication Facility, NorFab.

Authors' contributions

GB designed experiments. OS and GB conducted most of the experiments and wrote the article. KMP-A conducted NTA and AFM measurements and contributed to the manuscript. AS

contributed with experimental design and manuscript input. BTS contributed with writing the manuscript and were involved in discussions regarding NTA and AFM analysis. C-JA contributed with data interpretation/presentation and manuscript preparation. All authors read and approved the final manuscript.

Acknowledgements

The authors would like to thank the following for excellent technical assistance

Berit Størdal, Hann, Hella, Glenn Buene, Lill-Anny Gunnes Grøseth, Siri Backhe, Per Arne Aas and Nina-Beate Liabakk, Department of Clinical and Molecular Medicine, Faculty of Medicine, Norwegian University of Science and Technology (NTNU), Trondheim, Norway

The authors would also like to thank the following for assistance with figure preparation

Kirsten Strømme Kierulf-Vieira

Gunnar Anders Borthne

References

1. Borset M, Hjorth-Hansen H, Seidel C, Sundan A, Waage A. Hepatocyte growth factor and its receptor c-met in multiple myeloma. Blood. 1996;88(10):3998-4004.
2. Moschetta M, Basile A, Ferrucci A, Frassanito MA, Rao L, Ria R, et al. Novel targeting of phospho-cMET overcomes drug resistance and induces antitumor activity in multiple myeloma. Clin Cancer Res. 2013;19(16):4371-82.
3. Ro TB, Holien T, Fagerli UM, Hov H, Misund K, Waage A, et al. HGF and IGF-1 synergize with SDF-1alpha in promoting migration of myeloma cells by cooperative activation of p21-activated kinase. Exp Hematol. 2013;41(7):646-55.
4. Gambella M, Palumbo A, Rocci A. MET/HGF pathway in multiple myeloma: from diagnosis to targeted therapy? Expert Rev Mol Diagn. 2015;15(7):881-93.
5. Borset M, Lien E, Espevik T, Helseth E, Waage A, Sundan A. Concomitant expression of hepatocyte growth factor/scatter factor and the receptor c-MET in human myeloma cell lines. J Biol Chem. 1996;271(40):24655-61.
6. Blanquaert F, Pereira RC, Canalis E. Cortisol inhibits hepatocyte growth factor/scatter factor expression and induces c-met transcripts in osteoblasts. Am J Physiol Endocrinol Metab. 2000;278(3):E509-15.
7. Grano M, Galimi F, Zambonin G, Colucci S, Cottone E, Zallone AZ, et al. Hepatocyte growth factor is a coupling factor for osteoclasts and osteoblasts in vitro. Proc Natl Acad Sci U S A. 1996;93(15):7644-8.
8. Seidel C, Borset M, Turesson I, Abildgaard N, Sundan A, Waage A. Elevated serum concentrations of hepatocyte growth factor in patients with multiple myeloma. The Nordic Myeloma Study Group. Blood. 1998;91(3):806-12.
9. Andersen NF, Standal T, Nielsen JL, Heickendorff L, Borset M, Sorensen FB, et al. Syndecan-1 and angiogenic cytokines in multiple myeloma: correlation with bone marrow angiogenesis and survival. Br J Haematol. 2005;128(2):210-7.
10. Standal T, Abildgaard N, Fagerli UM, Stordal B, Hjertner O, Borset M, et al. HGF inhibits BMP-induced osteoblastogenesis: possible implications for the bone disease of multiple myeloma. Blood. 2007;109(7):3024-30.
11. Kristensen IB, Christensen JH, Lyng MB, Moller MB, Pedersen L, Rasmussen LM, et al. Hepatocyte growth factor pathway upregulation in the bone marrow microenvironment in multiple myeloma is associated with lytic bone disease. Br J Haematol. 2013;161(3):373-82.
12. Bataille R, Chappard D, Marcelli C, Dessauw P, Baldet P, Sany J, et al. Recruitment of new osteoblasts and osteoclasts is the earliest critical event in the pathogenesis of human multiple myeloma. J Clin Invest. 1991;88(1):62-6.
13. Giuliani N, Rizzoli V, Roodman GD. Multiple myeloma bone disease: Pathophysiology of osteoblast inhibition. Blood. 2006;108(13):3992-6.
14. van Niel G, Porto-Carreiro I, Simoes S, Raposo G. Exosomes: a common pathway for a specialized function. J Biochem. 2006;140(1):13-21.
15. Kowal J, Tkach M, Thery C. Biogenesis and secretion of exosomes. Curr Opin Cell Biol. 2014;29:116-25.
16. Bucki R, Bachelot-Loza C, Zachowski A, Giraud F, Sulpice JC. Calcium induces phospholipid redistribution and microvesicle release in human erythrocyte membranes by independent pathways. Biochemistry. 1998;37(44):15383-91.
17. Cocucci E, Racchetti G, Meldolesi J. Shedding microvesicles: artefacts no more. Trends Cell Biol. 2009;19(2):43-51.

18. Bobrie A, Colombo M, Raposo G, Thery C. Exosome secretion: molecular mechanisms and roles in immune responses. Traffic. 2011;12(12):1659-68.
19. Albanese J, Dainiak N. Modulation of intercellular communication mediated at the cell surface and on extracellular, plasma membrane-derived vesicles by ionizing radiation. Exp Hematol. 2003;31(6):455-64.
20. Aliotta JM, Pereira M, Johnson KW, de Paz N, Dooner MS, Puente N, et al. Microvesicle entry into marrow cells mediates tissue-specific changes in mRNA by direct delivery of mRNA and induction of transcription. Exp Hematol. 2010;38(3):233-45.
21. Valadi H, Ekstrom K, Bossios A, Sjostrand M, Lee JJ, Lotvall JO. Exosome-mediated transfer of mRNAs and microRNAs is a novel mechanism of genetic exchange between cells. Nat Cell Biol. 2007;9(6):654-9.
22. Anderson HC, Mulhall D, Garimella R. Role of extracellular membrane vesicles in the pathogenesis of various diseases, including cancer, renal diseases, atherosclerosis, and arthritis. Lab Invest. 2010;90(11):1549-57.
23. Purushothaman A, Bandari SK, Liu J, Mobley JA, Brown EE, Sanderson RD. Fibronectin on the Surface of Myeloma Cell-derived Exosomes Mediates Exosome-Cell Interactions. J Biol Chem. 2016;291(4):1652-63.
24. Derksen PW, Keehnen RM, Evers LM, van Oers MH, Spaargaren M, Pals ST. Cell surface proteoglycan syndecan-1 mediates hepatocyte growth factor binding and promotes Met signaling in multiple myeloma. Blood. 2002;99(4):1405-10.
25. Lyon M, Deakin JA, Lietha D, Gherardi E, Gallagher JT. The interactions of hepatocyte growth factor/scatter factor and its NK1 and NK2 variants with glycosaminoglycans using a modified gel mobility shift assay. Elucidation of the minimal size of binding and activatory oligosaccharides. J Biol Chem. 2004;279(42):43560-7.
26. Thery C, Amigorena S, Raposo G, Clayton A. Isolation and characterization of exosomes from cell culture supernatants and biological fluids. Curr Protoc Cell Biol. 2006;Chapter 3:Unit 3 22.
27. Psonka-Antonczyk KM, Hammarstrom P, Johansson LB, Lindgren M, Stokke BT, Nilsson KP, et al. Nanoscale Structure and Spectroscopic Probing of Abeta1-40 Fibril Bundle Formation. Front Chem. 2016;4:44.
28. Hjertner O, Torgersen ML, Seidel C, Hjorth-Hansen H, Waage A, Borset M, et al. Hepatocyte growth factor (HGF) induces interleukin-11 secretion from osteoblasts: a possible role for HGF in myeloma-associated osteolytic bone disease. Blood. 1999;94(11):3883-8.
29. Naka D, Ishii T, Shimomura T, Hishida T, Hara H. Heparin modulates the receptor-binding and mitogenic activity of hepatocyte growth factor on hepatocytes. Exp Cell Res. 1993;209(2):317-24.
30. Borawski J, Naumnik B, Mysliwiec M. Activation of hepatocyte growth factor/activin A/follistatin system during hemodialysis: role of heparin. Kidney Int. 2003;64(6):2229-37.
31. Ramani VC, Yang Y, Ren Y, Nan L, Sanderson RD. Heparanase plays a dual role in driving hepatocyte growth factor (HGF) signaling by enhancing HGF expression and activity. J Biol Chem. 2011;286(8):6490-9.
32. Seidel C, Borset M, Hjertner O, Cao D, Abildgaard N, Hjorth-Hansen H, et al. High levels of soluble syndecan-1 in myeloma-derived bone marrow: modulation of hepatocyte growth factor activity. Blood. 2000;96(9):3139-46.
33. Girasole G, Passeri G, Jilka RL, Manolagas SC. Interleukin-11: a new cytokine critical for osteoclast development. J Clin Invest. 1994;93(4):1516-24.
34. McCoy EM, Hong H, Pruitt HC, Feng X. IL-11 produced by breast cancer cells augments osteoclastogenesis by sustaining the pool of osteoclast progenitor cells. BMC Cancer. 2013;13:16.
35. Hughes FJ, Howells GL. Interleukin-11 inhibits bone formation in vitro. Calcif Tissue Int. 1993;53(5):362-4.

36. Cai WL, Huang WD, Li B, Chen TR, Li ZX, Zhao CL, et al. microRNA-124 inhibits bone metastasis of breast cancer by repressing Interleukin-11. Mol Cancer. 2018;17(1):9.
37. Raimondi L, De Luca A, Amodio N, Manno M, Raccosta S, Taverna S, et al. Involvement of multiple myeloma cell-derived exosomes in osteoclast differentiation. Oncotarget. 2015;6(15):13772-89.
38. Faict S, Muller J, De Veirman K, De Bruyne E, Maes K, Vrancken L, et al. Exosomes play a role in multiple myeloma bone disease and tumor development by targeting osteoclasts and osteoblasts. Blood Cancer J. 2018;8(11):105.
39. Umezu T, Tadokoro H, Azuma K, Yoshizawa S, Ohyashiki K, Ohyashiki JH. Exosomal miR-135b shed from hypoxic multiple myeloma cells enhances angiogenesis by targeting factor-inhibiting HIF-1. Blood. 2014;124(25):3748-57.
40. Liu Y, Zhu XJ, Zeng C, Wu PH, Wang HX, Chen ZC, et al. Microvesicles secreted from human multiple myeloma cells promote angiogenesis. Acta Pharmacol Sin. 2014;35(2):230-8.
41. Arendt BK, Walters DK, Wu X, Tschumper RC, Jelinek DF. Multiple myeloma dell-derived microvesicles are enriched in CD147 expression and enhance tumor cell proliferation. Oncotarget. 2014;5(14):5686-99.
42. Thompson CA, Purushothaman A, Ramani VC, Vlodavsky I, Sanderson RD. Heparanase regulates secretion, composition, and function of tumor cell-derived exosomes. J Biol Chem. 2013;288(14):10093-9.
43. Roccaro AM, Sacco A, Maiso P, Azab AK, Tai YT, Reagan M, et al. BM mesenchymal stromal cell-derived exosomes facilitate multiple myeloma progression. J Clin Invest. 2013;123(4):1542-55.
44. Wang J, Hendrix A, Hernot S, Lemaire M, De Bruyne E, Van Valckenborgh E, et al. Bone marrow stromal cell-derived exosomes as communicators in drug resistance in multiple myeloma cells. Blood. 2014;124(4):555-66.
45. Deng M, Yuan H, Liu S, Hu Z, Xiao H. Exosome-transmitted LINC00461 promotes multiple myeloma cell proliferation and suppresses apoptosis by modulating microRNA/BCL-2 expression. Cytotherapy. 2019;21(1):96-106.
46. Atai NA, Balaj L, van Veen H, Breakefield XO, Jarzyna PA, Van Noorden CJ, et al. Heparin blocks transfer of extracellular vesicles between donor and recipient cells. J Neurooncol. 2013;115(3):343-51.
47. Cossetti C, Iraci N, Mercer TR, Leonardi T, Alpi E, Drago D, et al. Extracellular vesicles from neural stem cells transfer IFN-gamma via Ifngr1 to activate Stat1 signaling in target cells. Mol Cell. 2014;56(2):193-204.
48. Li X, Wang S, Zhu R, Li H, Han Q, Zhao RC. Lung tumor exosomes induce a pro-inflammatory phenotype in mesenchymal stem cells via NFkappaB-TLR signaling pathway. J Hematol Oncol. 2016;9:42.
49. Taverna S, Pucci M, Giallombardo M, Di Bella MA, Santarpia M, Reclusa P, et al. Amphiregulin contained in NSCLC-exosomes induces osteoclast differentiation through the activation of EGFR pathway. Sci Rep. 2017;7(1):3170.
50. Webber J, Steadman R, Mason MD, Tabi Z, Clayton A. Cancer exosomes trigger fibroblast to myofibroblast differentiation. Cancer Res. 2010;70(23):9621-30.
51. Webber JP, Spary LK, Sanders AJ, Chowdhury R, Jiang WG, Steadman R, et al. Differentiation of tumour-promoting stromal myofibroblasts by cancer exosomes. Oncogene. 2015;34(3):290-302.

Figure legends

Figure 1. Characterization of EVs isolated from myeloma cell lines JJN-3 and INA-6. (A) Size distribution of EVs isolated from JJN-3 and INA-6 cells as measured by NTA (bin size 1 nm). Right upper corners of both NTA diagrams show EVs as point scatters undergoing Brownian motion (from recorded video). **(B)** AFM topographs of EVs derived from JJN-3 cells (left) and INA-6 cells (right). **(C)** Immunoblot analysis of EV-markers CD9, ALIX and LAMP-1, and the cellular marker PDI, in lysates of cells and EVs. C: total cell lysate; EV: extracellular vesicle lysate. Molecular weights are shown in kilodalton. **(D)** EVs isolated from JJN-3 and INA-6 cells were analyzed with silverstained protein gels, showing similar protein expression levels. **(E)** Cell status before EV isolation from JJN-3 and INA-6 cells as evaluated by flow cytometry. The cells were analyzed by annexin V fluorescein isothiocyanate (FITC) and propidium iodide (PI) staining, and double-negative cells were considered viable (lower left quadrants).

Figure 2. Myeloma-derived EVs mediate HGF/c-Met signaling in osteoblast-like cells.

(A) Concentration of HGF in EV-isolates obtained from HGF-secreting JJN-3 and non-HGF-secreting INA-6 cells as measured by ELISA. **(B)** ELISA measurement of IL-11 in U2OS culture medium after incubation with EVs from JJN-3 and INA-6 cells. Two EV-concentrations were used (1× and 3×). Induction of IL-11 secretion was observed with JJN-3-derived EVs only, in a dose dependent manner. A c-Met inhibitor was added to U2OS cells before exposure to either recombinant human HGF (hrHGF) or JJN-3-derived EVs (3×). In the presence of c-Met inhibitor, EV-induced IL-11 secretion was reduced to background levels. As positive control, hrHGF was used and elicited a strong IL-11 response, which was partially abrogated with the use of c-Met inhibitor. To exclude soluble HGF as the cause of IL-11 induction, the supernatant

from the last ultracentrifugation step when isolating JJN-3-derived EVs was used and showed background IL-11 levels. **(C)** IL-11 measurement after heparin treatment of bead-bound EVs. Heparin-treated bead-bound EVs result in significantly lower Il-11 culture media levels than non-treated bead-bound EVs. Magnetic beads only were used as negative control. **(D)** IL-11 levels in Saos-2 culture media as measured with ELISA. Saos-2 cells were incubated with JJN-3-derived EVs in two concentrations (1x and 3x). Culture media from non-stimulated Saos-2 cells were used as a negative control. A c-Met inhibitor was added to Saos-2 cells before addition of JJN-3-derived EVs (3×). As positive control, hrHGF was used in three different concentrations. To exclude soluble HGF as the cause of EV-mediated IL-11 induction, the supernatant from the last ultracentrifugation step when isolating JJN-3-derived EVs was used. ELISA results are based on two independent experiments, each with three parallels. Data are presented as mean with standard deviation.

Figure 3. Schematic overview of mechanisms of HGF/c-Met signaling. (A) HGF may signal through association to proteoglycans on the cell surface. **(B)** HGF may signal as soluble ligand. **(C)** HGF may signal through a complex with the proteoglycan Syndecan-1. **(D)** As demonstrated in the present article, HGF may also signal through association to proteoglycans on the EV surface.

Figure 4. HGF concentrations for MM-patient derived EVs and MM-patient BMP as measured by ELISA. A) HGF concentrations for BMP-derived EV isolates for fifteen MM patients. EV-isolates for patient 10-16 and 18-19 express HGF below the assay's detection limit of 3 pg/ml. Analyses were performed in duplicates. **(B)** HGF concentrations in BMP for the same fifteen patients. Analyses were performed in duplicates. **(C)** HGF concentrations for EVs isolated from cultured primary MM cells from six of the fifteen patients. Cells were grown for 72 hours before EV-isolation. Only EVs from patient 8 express HGF

at values above the assay's detection limit for all parallels. Analyses were performed in triplets. All data are presented as mean with range.

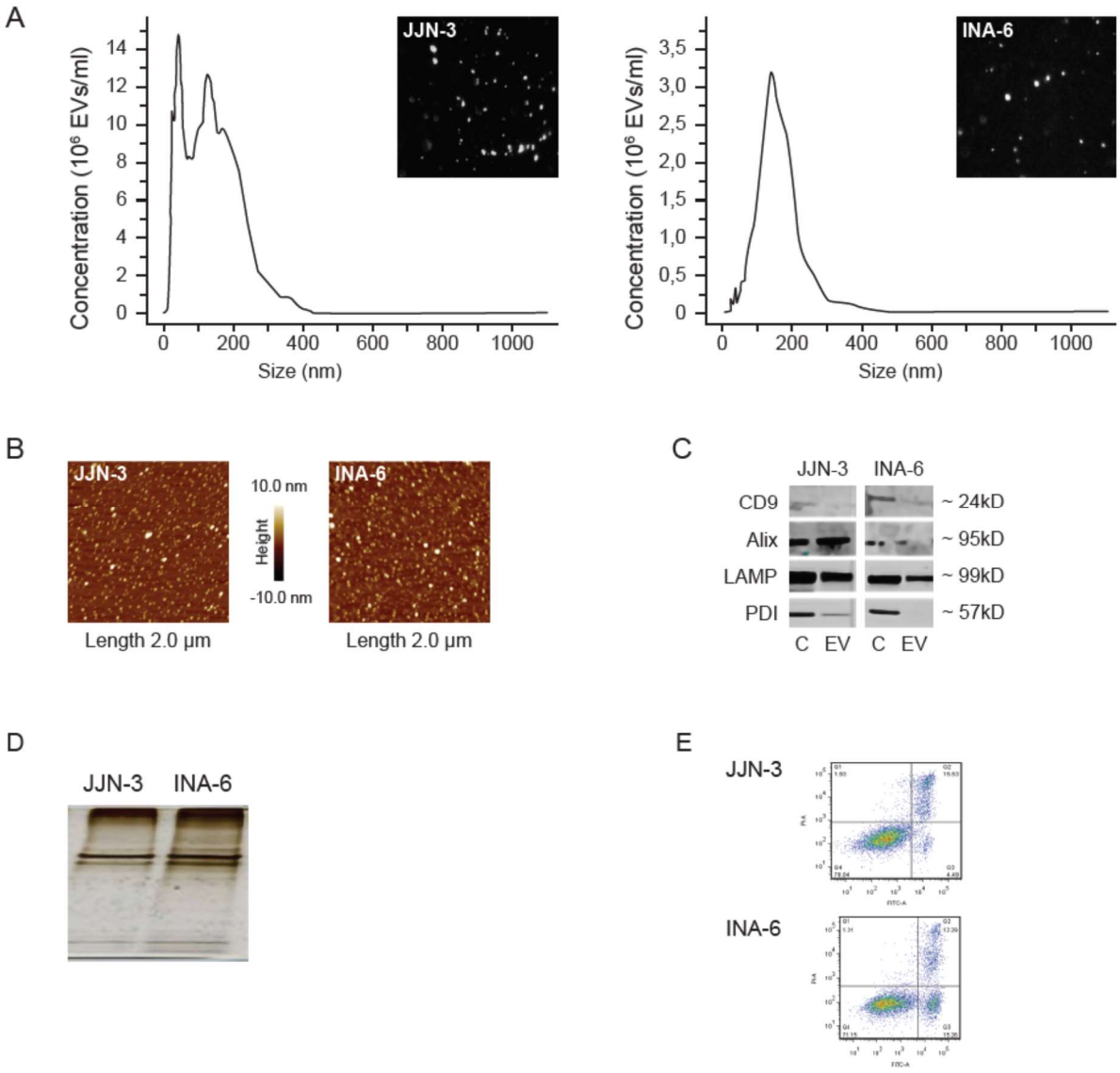
A
JJN-3
Concentration (10⁶ EVs/ml)
Size (nm)
INA-6
B
JJN-3
10.0 nm
Height
-10.0 nm
INA-6
Length 2.0 µm
Length 2.0 µm
C
JJN-3
INA-6
CD9
Alix
LAMP
PDI
~ 24kD
~ 95kD
~ 99kD
~ 57kD
C EV C EV
D
JJN-3
INA-6
E
JJN-3
INA-6

Figure 1

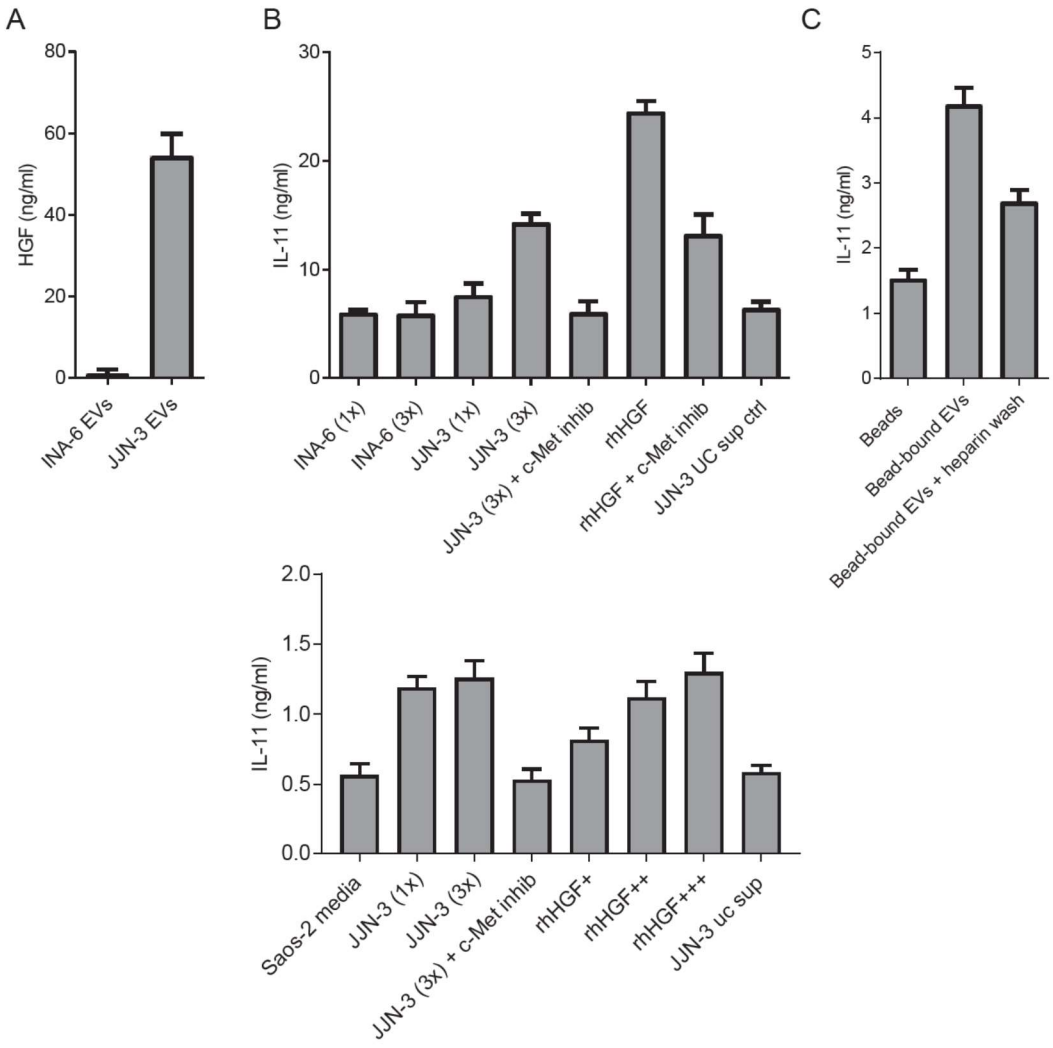
A
HGF (ng/ml)
80
60
40
20
0
INA-6 EVs
JJN-3 EVs
B
IL-11 (ng/ml)
30
20
10
0
INA-6 (1x)
INA-6 (3x)
JJN-3 (1x)
JJN-3 (3x)
JJN-3 (3x) + c-Met inhib
rhHGF
rhHGF + c-Met inhib
JJN-3 UC sup ctrl
C
IL-11 (ng/ml)
5
4
3
2
1
0
Beads
Bead-bound EVs
Bead-bound EVs + heparin wash
IL-11 (ng/ml)
2.0
1.5
1.0
0.5
0.0
Saos-2 media
JJN-3 (1x)
JJN-3 (3x)
JJN-3 (3x) + c-Met inhib
rhHGF+
rhHGF++
rhHGF+++
JJN-3 uc sup

Figure 2

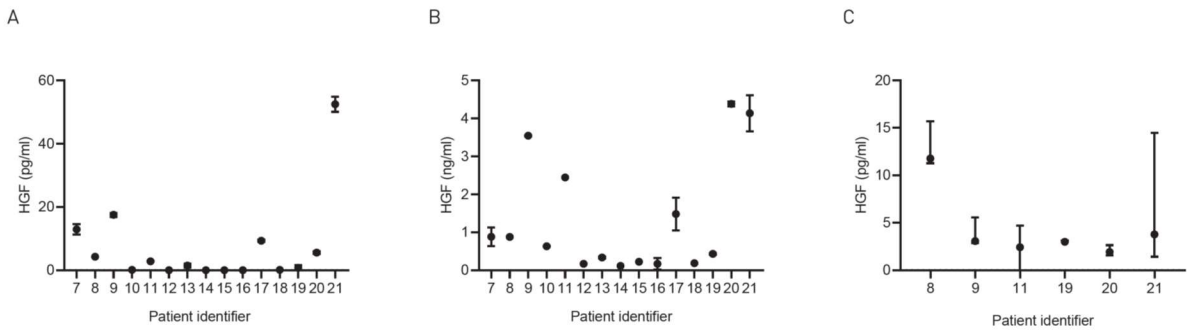

Figure 3

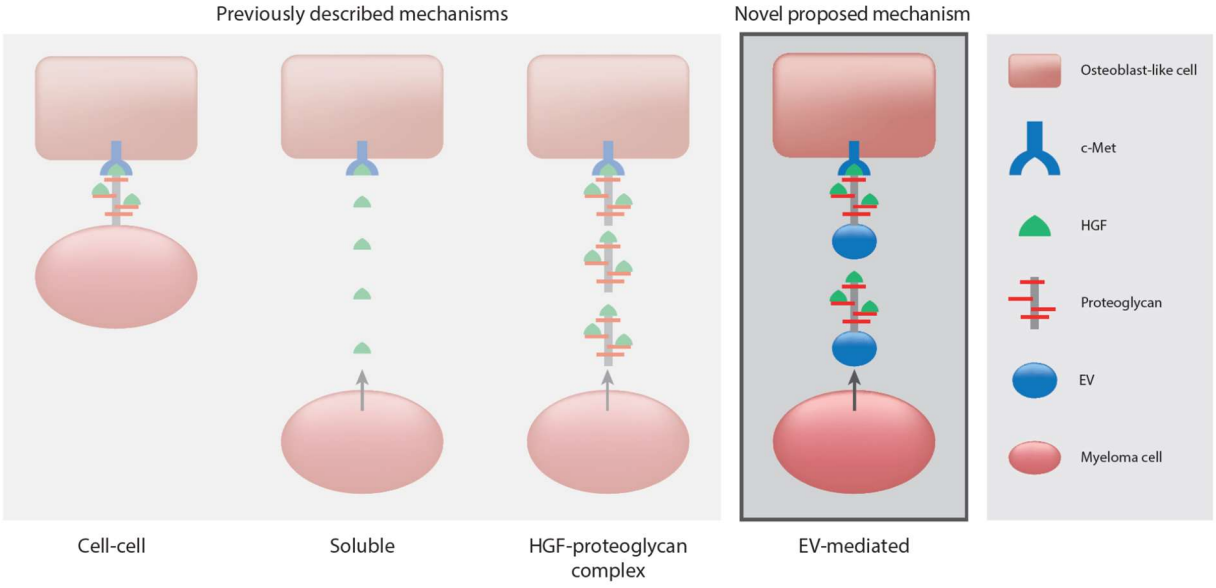

Figure 4